

## Water on surfaces studied by scanning probe microscopies

Albert Verdaguer<sup>1\*</sup>, Aitor Mugarza<sup>1</sup>, Jordi Fraxedas<sup>2</sup>

1. Institut Català de Nanotecnologia (ICN)
2. Centre d'Investigacions en Nanociència i Nanotecnologia (CIN2, CSIC-ICN)

### Resum

La manera com es mulla una superfície quan se l'exposa a l'aigua determina fenòmens crucials en biologia, en química i en ciència de materials. Les microscòpies locals de rastreig han obert recentment nous camins per a estudiar capes i gotes d'aigua sobre superfícies que han permès l'estudi de les propietats d'allò mullat a nivell molecular. S'han desenvolupat diverses vies d'aproximació utilitzant aquestes tècniques que proporcionen diferents informacions sobre el fenomen del que és mullat. Per exemple, la microscòpia de rastreig d'efecte túnel s'utilitza per estudiar l'estructura de petits clústers i monocapes de molècules d'aigua absorbides en superfícies. Malauradament, aquests estudis estan limitats a temperatures criogèniques i per substrats conductors. Per investigar fenòmens relacionats amb allò mullat en condicions ambientals, el microscopi de forces atòmiques en modes electrostàtics de no-contacte ha esdevingut una eina molt poderosa. Mitjançant aquesta tècnica s'estudia l'estructura de les capes d'aigua més enllà de la primera monocapa, es poden obtenir imatges de gotes a escala nanomètrica per investigar la hidrofobicitat i la hidrofilitat a escala molecular, s'investiguen processos químics dins de capes d'aigua o s'intenta millorar la impermeabilitat de recobriments moleculars utilitzats en nanotecnologia. En aquest article es presenta una selecció d'estudis il·lustratius, realitzats mitjançant microscòpies locals de rastreig, sobre diferents aspectes rellevants en ciència i tecnologia relacionats amb l'aigua i les superfícies.

Paraules clau: microscòpia de sonda de rastreig (SPM) · microscòpia de força atòmica (AFM) · microscòpia d'efecte túnel (STM) · aigua en superfícies · interaccions hidrofòbiques i hidrofíliques a nivell molecular

### Abstract

The wetting properties of a surface exposed to water determine crucial phenomena in biology, chemistry and material sciences. Scanning Probe Microscopies have recently opened new ways to study water films and droplets on surfaces allowing the study of the wetting properties of surfaces at molecular level. Several approaches providing different information on the phenomena have been developed. Scanning Tunneling Microscopy is being used to study the structure of water clusters and water monolayers, but unfortunately these studies are limited to low temperatures and conductive substrates. Atomic Force Microscopy working in non-contact electrostatic modes has become a powerful tool to investigate wetting in ambient conditions. This technique is being used to study the structure of water films beyond the first monolayer, imaging droplets at the nanometer range to study hydrophobicity and hydrophilicity at molecular level, studying chemical processes within adsorbed water films or probing the impermeability of molecular coatings used in nanotechnology. A selection of illustrative Scanning Probe Microscopy studies covering different scientific and technologically relevant aspects related to water and surfaces on water is presented in this review.

Keywords: scanning probe microscopy (SPM) · atomic force microscopy (AFM) · scanning tunneling microscopy (STM) · water on surfaces · hydrophobic and hydrophilic interactions at molecular level.

### Introduction

Any surface under ambient conditions is covered by a thin film of water. This film can be a fraction of a monolayer, many molecular layers or even a macroscopic film that can be seen with the naked eye. Unless in very high humidity conditions, where macroscopic films and droplets can form on surfaces, the

\* Author for correspondence: Albert Verdaguer. Centre d'Investigacions en Nanociència i Nanotecnologia (CIN2) (CSIC-ICN), Campus de la UAB, Edifici CM-7. E-08193 Bellaterra, Barcelona, Catalunya, EU. Tel. +34 934813722. Fax +34 935813717. Email: Albert.Verdaguer.ICN@uab.es

thicknesses scale of water films are generally nanometers. Yet such a thin film can have strong effects on the chemical and physical properties of the substrate surface.

The thickness of the film will depend not only on the ambient conditions but also on the wetting properties of the surface. The structure of the water molecules at the water-substrate interface determines their wetting properties and underlies the vast array of phenomena known under the names of hydrophobicity (nonwetting) and hydrophilicity (wetting), which describe the interaction between objects in aqueous media. These phenomena are crucial in biology and in material sciences.

There are many fundamental questions on the nature of thin films of water that still need in-depth investigation. The thickness of water films and the structure of water molecules in the film, amorphous or ordered, are still unknown for many important surfaces. Both parameters will affect the thermodynamic properties of the surface and how the whole system interacts with the environment. Important chemical reactions involving molecules from the surface or molecules present in the environment can happen within a water film on a surface. This chemistry can be very different from chemistry in bulk water and it is still not well understood. Interactions between surfaces change when water films are present; water films play a key role in friction and adhesion forces between surfaces. It is therefore not surprising that the study of interfacial water structure continues to be a subject of great interest and that many studies are devoted to it. Several excellent reviews exist that extensively cover the large body of literature published in recent years [1, 2].

To study liquid films of nanometer dimensions, instruments with nanometer resolution are needed. Several techniques that have nanometer resolution in the direction perpendicular to the surface can be used to study water films on surfaces. The Surface Force Apparatus can measure the interaction forces between two surfaces through a liquid [3], infrared spectroscopy and ellipsometry are used to measure the thickness of thin films [4] and X-ray diffraction has been used to study the structure of films, interfaces and surfaces [5]. Recently the development of X-ray photoemission at ambient pressures has opened new ways to study thicknesses and structures of water films on surfaces [6].

However, all these techniques have a common problem; they provide poor lateral resolution, in the order of microns at best. Understanding wetting at smaller lateral scales is important in many applications, since most wetting related phenomena depend on local properties of the surfaces such as defects. In nanotechnology, when dealing with nanofabricated devices and nanoparticles and their wetting properties, having nanometer lateral resolution becomes a must.

This need has been fulfilled thanks to the development of scanning probe microscopy (SPM) techniques, in particular, the atomic force microscope (AFM) and the scanning tunneling microscope (STM) [7]. In this article we shall review the SPM techniques used in the study of different aspects of the interaction of water films and surfaces. We will devote particular attention to studies at ambient conditions using a non contact AFM

method called Scanning Polarization Force Microscopy as a powerful tool to image liquids at the nanoscale. We will also discuss STM studies of water structures on surfaces at low temperature.

## Low temperature water structures studied by STM (Water on metals)

A) Adsorption structure of water on metals: from monomers to a monolayer structure.

A bottom-up approach to study the growth of water structures on a surface can be followed up by observing the interaction between single water molecules when the first intermolecular bonds start to form. The interplay between water-substrate interaction and the possible energy gain by forming H-bonds with neighboring molecules will determine the final structure. Since the strengths of these two interactions are comparable, variations in substrate chemical nature, surface geometry, or thermal conditions may lead to very different structures. Low temperature STM is an ideal tool for investigating surface structures with molecular resolution. In addition to determining the surface structure by imaging, it provides an opportunity to manipulate individual adsorbates with the tip and to perform chemistry in a controlled fashion [8]. A necessary condition for STM is the need for a conducting substrate, and for this reason most STM studies have been limited to metal surfaces.

The first step is to study the adsorption of isolated single water molecules. This requires low temperature and low coverage in order to limit the aggregation of the molecules into clusters as a result of the high diffusivity of single molecules. According to density functional theory (DFT) calculations, it was found that, in general, the favored adsorption site of a water monomer (single water molecule) is on top of the metal atoms and the optimal geometry is the one where the plane of the water molecule lies almost parallel to the surface [9]. On-top adsorption geometry has been experimentally observed on several metals [10, 11]. The calculated adsorption energies are fairly low, varying from 0.13 eV in Au(111) to 0.42 eV in Rh(111). This bonding strength is in the weak chemisorption/physisorption limit and, as mentioned above, the characteristic bonding energy of 0.25 eV of an H-bonded water molecule lies within the same energy range.

The aggregation of water molecules into clusters was initially studied using vibrational spectroscopic techniques [1]. Based on these results, monomers and small clusters, from dimers to hexamers, have been proposed to exist on metal surfaces. However, the first solid experimental evidence was provided by the real space visualization by STM. The diffusion and aggregation of water molecules studied on Pd(111) at temperatures below 60 K represents a good example [10]. Here it was found that dimers, trimers, tetramers and larger clusters could be formed by successive addition of colliding molecules (Figure 1). An unexpected result of these studies was that the mobility of the dimers, trimers and tetramers was higher than that of the monomers by several orders of magnitude. The cluster mobility

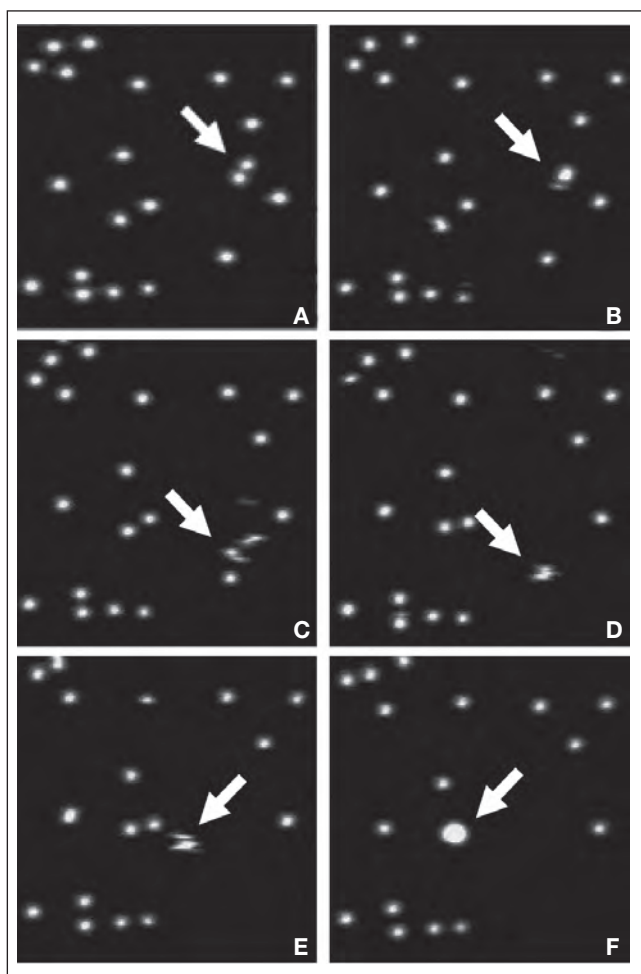


Figure 1. Sequence of images showing water molecules adsorbed on Pd(111) at 40K. Two monomers in (a) join to form a dimer in (b). The dimer diffuses faster than the scanning speed so that the tip scans over the molecule for one line before moving to a neighboring site and produces the streak in (c). The dimer encounters a third monomer and forms a trimer in (d), which diffuses approaching a pair of nearby monomers in (e). A pentamer is formed by the collision in (f). (Adapted from Ref. [10]).

decreased again to a value similar or smaller than that of the monomer when the clusters reached a size of five or more molecules. The authors proposed that the large mobility of the small clusters is due to the strong H-bonding between molecules, and to the mismatch between the O-O distance in the clusters and the lattice constant of Pd(111). In this model the mismatch would prevent both molecules from forming bonds to the substrate in optimal geometries, thus reducing the diffusion barrier of the cluster.

Mismatch between the O-O distances in H-bonded water molecules and the lattice constant of the metal is not only important for diffusion but can also play a key role in the stabilization of certain structures in the first water monolayer [12]. A particularly stable cluster of water on metal surfaces is the cyclic hexamer, which is the basic structure that can be found in hexagonal ice  $I_h$ . Hexamers were indeed found to constitute the building block for the formation of the first water layer on metals. The structure of isolated hexamers, however, might differ appreciably from that in ice  $I_h$ , depending on the strength of the water-substrate interaction and on the mismatch between

the substrate lattice constant and water molecule oxygen distances. The internal molecular structure of water hexamers on Ag(111) and Cu(111) are a good example of the competition between these two interactions [13],[14]. The mismatch between Ag(111) lattice constant and O-O distance in crystalline ice  $I_h$  is of ~5%, the metal lattice constant being larger. In spite of this, hexamers showed a perfect accommodation to the silver lattice constant, indicating considerable stretching of the H-bonds compared to hydrogen bonds in ice  $I_h$ . On the other hand, the mismatch in Cu(111) points in the opposite direction: the distance between Cu atoms is ~8% lower compared to the O-O distances in  $I_h$ . The hexamers observed on this surface deviate considerably from a high symmetry hexagon and show different H-bond lengths within the hexamer. In addition, the apparent height of the molecules within the hexamer is not alternating as in the ice bilayer. This leads to the formation of hexagons where not all molecules are adsorbed in identical positions, explaining the variety of apparent heights that are observed with STM. Therefore, in the competition between ideal hydrogen bond lengths and favorable on-top positions, it appears that none of them clearly dominates on the Cu(111) surface. Moreover, by comparing the results on the two surfaces one can conclude that it is easier to expand a hexamer than to compress it.

Until recent years most experimental results for water layers on metals were interpreted according to a model where the water monolayer adopts the structure of the puckered honeycombs found in the basal plane of ice  $I_h$ . The monolayer was found in many cases to be in registry with the surface lattice of fcc(111) and hcp(0001) metals, based in part on low energy electron diffraction (LEED) observations [1]. It had been commonly accepted that the hydrogen atoms that are not part of an H bond pointed up and perpendicularly to the surface, in what is called the H-up configuration. The first STM studies of monolayers on Pt(111), Ag(111) and Cu(111) were also interpreted following this model. However, the interaction of the water molecules with the surface atoms can result in deviations from this optimum structure, leading to novel structures not found in bulk ice. This was indeed observed on the growth of the first monolayer of water on Pd(111), where flat hexamer units ordered in quasi 2D interconnected chains [15], as can be seen in Figure 2. Interestingly the growth of these clusters is limited to a few unit cells. Addition of more water to the surface either leads to the nucleation of more clusters of similar size, or produces second layer structures. The STM images indicate a constant tunneling probability on each corner of the hexagonal cell where water is located, except at the periphery of the islands. This observation was interpreted as indicating that the water molecules are in the same chemical and geometrical state inside the cluster, unlike in the case of the molecules in the puckered hexagons of the  $I_h$  structure. Based on these results a model was proposed where the molecules are nearly coplanar and use all their H atoms to form bonds with neighboring molecules, while bonding to the substrate through the lone pair orbitals. This model necessarily implies that the cluster size must be limited to a few cells, since in two dimensions only a finite number of molecules can be fully H-bonded (dou-

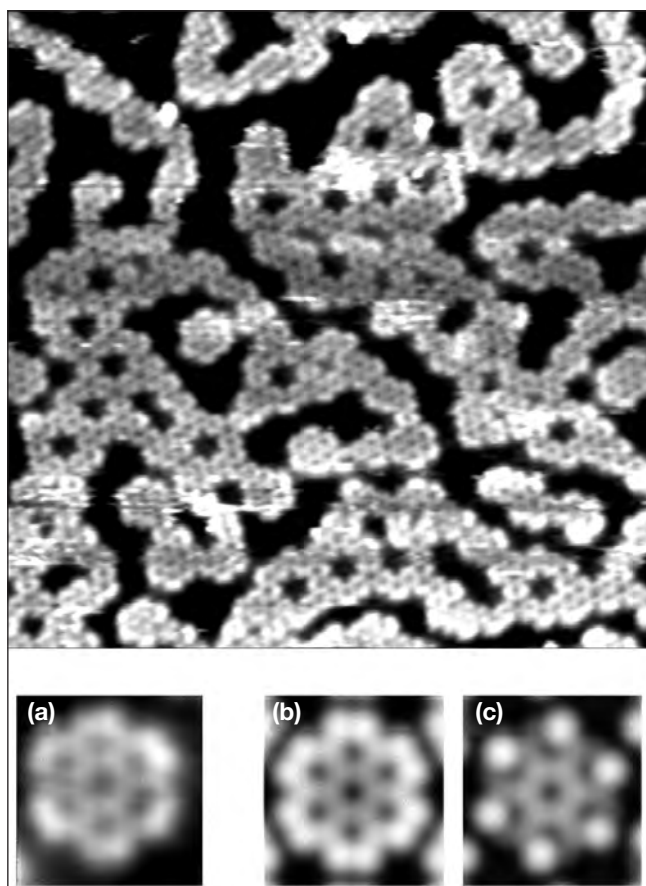


Figure 2. Top: ( $175 \text{ \AA} \times 175 \text{ \AA}$ ) STM image of  $\text{D}_2\text{O}$  clusters on Pd(111) at 100 K. The growth of the hexagonal honeycomb clusters is limited to a few unit cells in one direction. Bottom:  $\text{D}_2\text{O}$  clusters on Pd(111) at 100 K. Bottom: (a) Experimental STM images of a “rosette” structure made up of 7 hexagons. (b), (c) STM topographic image simulations for two different DFT-optimized models of the rosette structure. In (b) the edge water molecules have an H-down configuration. In (c) alternating molecules are dissociated to OH (a similar simulated image was obtained from an H-up configuration). Clearly (b) matches much better with experimental image (a). (Adapted from Ref. [15])

ble donors, single acceptor, and a 4th bond to the substrate). It is the peripheral molecules that contain the unsaturated bonds, either dangling H atoms sticking out towards the vacuum, or directed to the Pd underneath, or perhaps with the H-bond broken to form OH. DFT calculations were carried out to determine which of these three possibilities is more stable. Although the optimized geometries did all produce flat, undissociated, and fully H-bonded molecules inside the clusters, the energies for the three peripheral geometries (H-up, H-down, OH) were too close in value to decide which model was most likely. The answer was found through a comparison of the calculated STM images for each configuration with the experimental one. As shown in Figure 2, only the model with peripheral molecules in an H-down configuration produced STM images that closely matched the experiments.

As the water coverage on the surface increases over the monolayer, different structures will be formed depending on the relative strength of water-water interaction in a layer and across layers: if the former dominates flat multilayers will grow (wetting case), whereas in the opposite case three-dimensional islands will grow (non-wetting case).

## B) Stability of water upon dissociation and the effect of coadsorbates

The ice bilayer model was first challenged by experimental and theoretical work on the growth of water on Ru(0001). In a LEED study of  $\text{D}_2\text{O}$  on Ru(0001) a honeycomb structure in registry with the surface atoms was indeed observed, but a careful analysis of the spot intensities indicated that on this surface the O atoms in  $\text{D}_2\text{O}$  are nearly coplanar [16]. The result, at odds with the puckered ice bilayer model, motivated theoretical analysis of the energetics of water adsorption [17]. It was found that the binding energy of the undissociated monolayer was less than the energy formation of bulk ice, which means that the monolayer should not be stable and should therefore dewet the surface to form three-dimensional ice crystals. A different model was proposed where alternating water molecules (those not attached to the substrate in the original ice-like bilayer) dissociate into OH and H, with the O in the OH groups bonding covalently to the metal and forming a quasi-planar layer. Nevertheless, most experiments on Ru(0001) suggested intact, undissociated adsorption of water at low temperature. The explanation for this controversy is the high energy barrier needed to dissociate the metastable intact water, which is comparable to the desorption energy [18]. This implies a competition between the thermally activated dissociation and desorption, which in turn explains the double peak observed in thermal desorption spectroscopy (TDS) experiments [19].

But the real structures related to both the intact and the partially dissociated phases have only been revealed very recently by STM. The low temperature phase of intact water appears to be a 2D, flat honeycomb structure [20], as can be observed in Figure 3 (a). Similar to Pd(111), a second layer starts to form before completely wetting the surface, probably due to the same lateral limitations related to the tendency of water to grow coplanar using all their H atoms. Surprisingly, after annealing above the desorption temperature of 160 K observed for intact water, the structures suffer a dramatic change, becoming 1D chain structures of limited size and with a brighter contrast at the perimeter (see Figure 3 (b)). The structural change was related to the partial dissociation of water. Additional experiments on an Ru(0001) surface covered with 0.03 ML of C impurities showed the same chain structures with a higher resolution, as can be seen in Figure 3 (c). In this case the internal structure could be revealed, indicating that the chains consist of flat, linearly connected hexamers, surrounded by molecules of brighter contrast at the perimeter. STM simulation images on this system helped identify all observed species formed upon dissociation of water on this surface [11]. One important finding was that outside the clusters, H and CH coexisted with the initial C impurities, as can be observed in Figure 3 (c). This can be explained by H being spilled out from the partially dissociated water clusters and CH being formed by reaction of the former with the pre-existing C, which provides the first real spatial evidence for water dissociation on Ru(0001). The best fit between STM images and simulations of the different linear chains observed are obtained with mixed  $\text{H}_2\text{O}$  and OH with ratios varying from 4:0 to 5:3 [20].



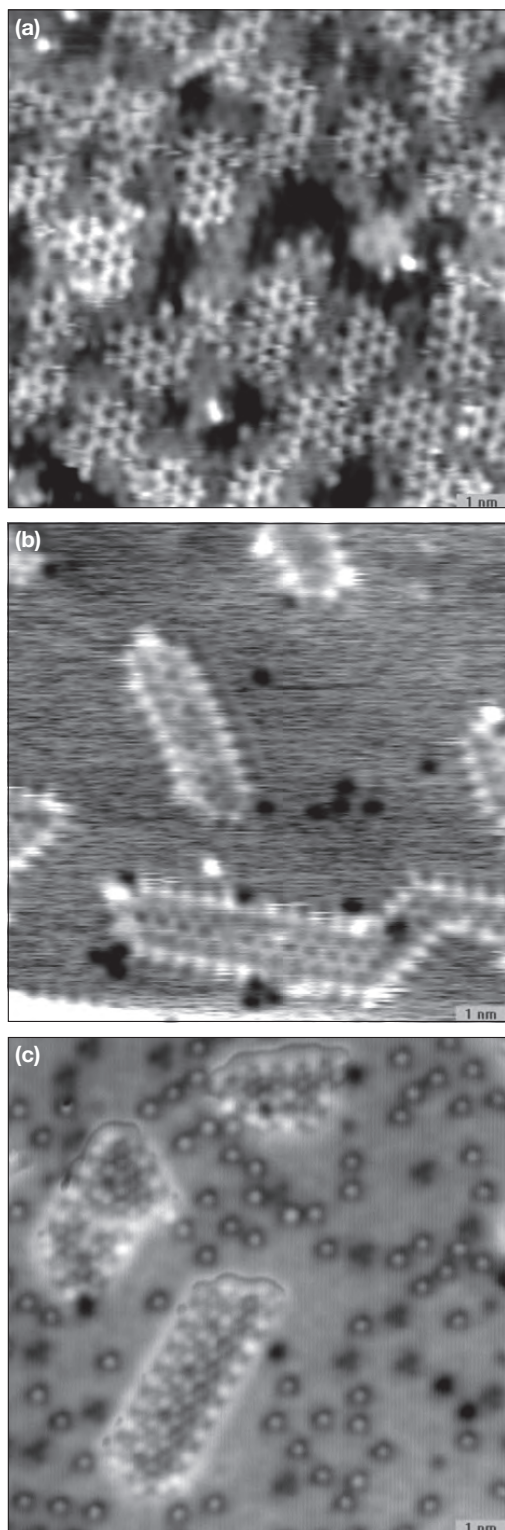


Figure 3. STM images of water adsorption at (a) low temperature and (b) after annealing above 165 K. At low temperature, intact water grows forming hexagonal honeycomb clusters. A second layer grows on top before completely wetting the surface. Above 165 K, 1D chains of limited size with a bright perimeter can be observed, which correspond to a partially dissociated phase consisting of mixed  $\text{H}_2\text{O}$  and OH molecules. (c) A high resolution image of a structure similar to the ones observed in (b), obtained after dosing water on a Ru(0001) surface containing 0.03 ML of C impurities and annealing above 140 K. The internal structure reveals a 1D hexagonal honeycomb structure surrounded by a perimeter of brighter contrast. Outside the cluster H atoms (circular depression) released from the clusters are observed, and most of the pre-existing C (triangular depression) react with the H to form CH (triangular depression with a bright protrusion in the center).

The effect of C on the growth and stability of water is double: it prevents the growth of long-range ordered honeycomb networks by site-blocking, and it lowers the energy barrier so that partial dissociation starts already at 140 K. A similar stabilization of the partially dissociated phase was also observed for water coadsorption with O for a coverage of the latter smaller than 0.25 ML [21, 22]. A strikingly different behavior is observed, however, for a coverage above 0.25 ML, where the O stabilizes the intact phase up to the desorption temperature of 220 K. At this O coverage a  $2 \times 2$  superstructure is formed, and a combined study of STM and DFT calculations showed that water on this surface adsorbs on top sites with the O-H axis parallel to the surface, similar to the configuration on the clean surface, but forming two additional H bonds to the neighboring O atoms [23]. The adsorption configuration is illustrated in Figure 4, together with STM images confirming the calculated adsorption site. The H bonds stabilize the intact water monomer by lowering the adsorption energy by 220 meV and blocks the formation of the honeycomb structures observed on the clean surface. Yet the main reason for the quenching of dissociation in the unfavorable adsorption energy of the dissociation products, H and OH, in this O-covered surface [24]. As the water coverage increases up to 0.25 ML, an intercalated  $2 \times 2$  water and O superstructure is formed, as can be seen in Figure 4 (b).

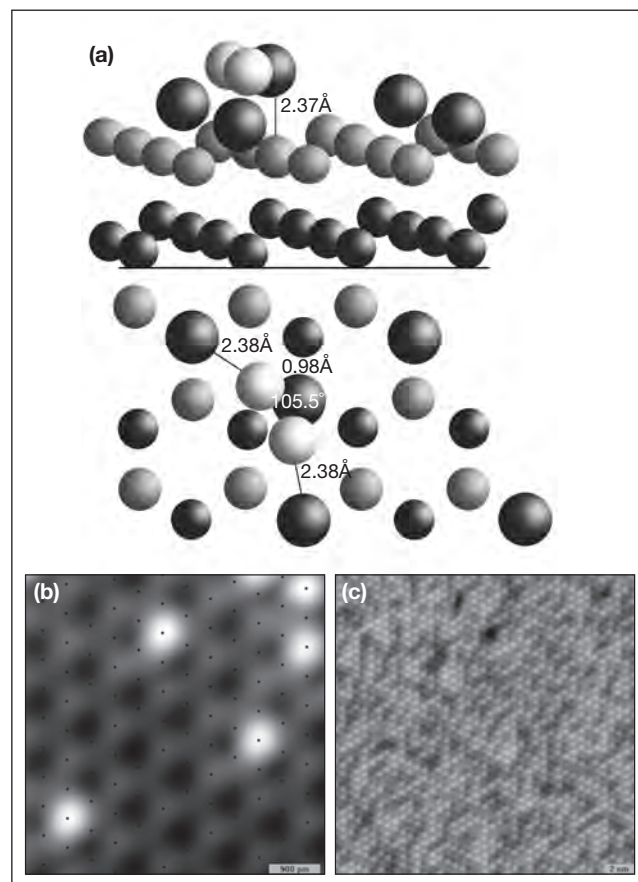


Figure 4. (a) Adsorption configuration of a water monomer on the  $\text{O}(2 \times 2)/\text{Ru}(0001)$  surface obtained by DFT. (b) STM image showing water monomers adsorbing on the top sites that are not blocked by the O (blue dots represent the  $1 \times 1$  grid of top sites), as theory predicts. (c) STM image for a higher coverage of water (0.18 ML), where the intercalated  $2 \times 2$  structure of O and water can be observed.

## Non-contact AFM modes to study liquids on surfaces

Among the microscopy tools with nanoscale lateral resolution that can operate under ambient conditions, AFM is one of the most versatile. A large number of publications report AFM studies of the effect of water on surface properties such as adhesion, friction, dissolution, oxidation and hydroxylation [1]. In most cases the AFM tip is directly in contact with the surface, which strongly perturbs the liquid film.

Different non-contact AFM methods have been used to study liquid films and droplets. For liquids of low viscosity it is easy, even when using non-contact methods, to perturb the film. In many AFM methods, the cantilever is set to oscillate with an amplitude that causes the tip to either briefly contact, or to come very close to the surface. While this eliminates the friction and dragging effects that occur in contact mode, the brief interaction between tip and liquid surface can still result in perturbations that need to be considered. Scanning polarization force microscopy (SPFM) overcomes many of these problems and provides, in addition to surface topography, information on other surface properties, such as local variations in the surface potential and ionic mobility [24]. SPFM is based on electrostatic forces between the tip and the surface and can be applied to both conductive and non-conductive substrates. The principle of operation is shown in Figure 5. A bias voltage in the order of a few volts is applied to a conductive tip. Opposite charges at the tip and the surface arising from the polarizability of the materials create attractive electrostatic forces that bend the tip towards the surface. Because electrostatic forces have a long range, they provide a means of imaging at distances of several nanometers. The disadvantage is that the large tip-to-sample-distance results in a lower spatial resolution, to the order of the tip sample distance or the tip radius. On the positive side, the large separation between tip and sample makes it possible to reduce the perturbation of the liquid surface to a

negligible value. The vertical resolution of SPFM is not as negatively influenced by the large tip-to-sample-distance and is typically in the angstrom region, comparable to that of other AFM modes. The electrostatic force can be written as follows:

$$F_e(V) = aV^2 + bV + c$$

where a,b,c are factors that depend on the geometry of the system (tip radius and shape, etc.) and the local dielectric constant at the surface. The first contribution ( $aV^2$ ) is due to the polarization of the sample and tip (induced charges). The remaining terms contain the interaction between the biased tip and charges or dipoles that are not induced by the bias voltage on the tip and are located at the surface. If an ac voltage  $V = V_{dc} + V_{ac} \sin(\omega t)$  is applied to the tip, the frequency  $\omega$  can be varied to explore time-dependent phenomena. Using lock-in amplifiers tuned to the second and first harmonic of the modulation signal, respectively, the electrostatic force components  $F(2\omega)$ ,  $F(\omega)$  can be measured separately.  $F(2\omega)$  contains information on the polarizability (dielectric constant) and topography. The contact potential contribution to the electrostatic force can be determined from the first harmonic of the lever oscillation (i.e.  $F(\omega)$ ).  $F(\omega)$  is nullified by a feedback bias voltage that enables us to measure the real contact potential of the surface as in the Kelvin Probe method. This mode is called Kelvin Probe Microscopy (KPM) and gives information about dipoles and charges on the surfaces [7].

## Water film structure induced by the substrate (water on mica)

For years there has been a particular interest in the study of water adsorption on surfaces that can induce ice nucleation, especially at temperatures above 0°C. This idea lies behind the attempt to influence weather and to produce substances that,

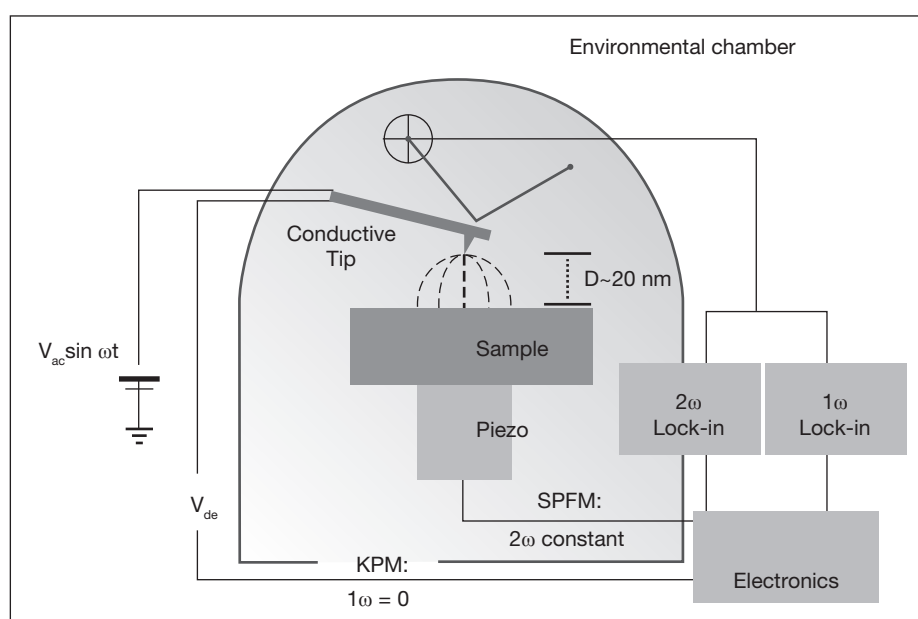


Figure 5. Illustration of the principle of operation of Scanning Polarization Force Microscopy (SPFM). A low voltage is applied to a conductive cantilever and tip of the Atomic Force Microscope. Induced charges at the tip and surface create attractive electrostatic forces that bend the tip towards the surface. An ac voltage  $V = V_{dc} + V_{ac} \sin(\omega t)$  is applied to the metallic tip. Using lock-in amplifiers the second and first harmonics of the modulation frequency are measured separately in the electrostatic force. To separate the contributions of topography and the contact potential distribution at the surface, two feedback loops are used. The first maintains the amplitude of  $F(2\omega)$  constant by adjusting the tip-sample distance. The second adjusts the applied  $V_{dc}$  bias so that  $F(\omega)$  is zero, as in the Kelvin Probe method.

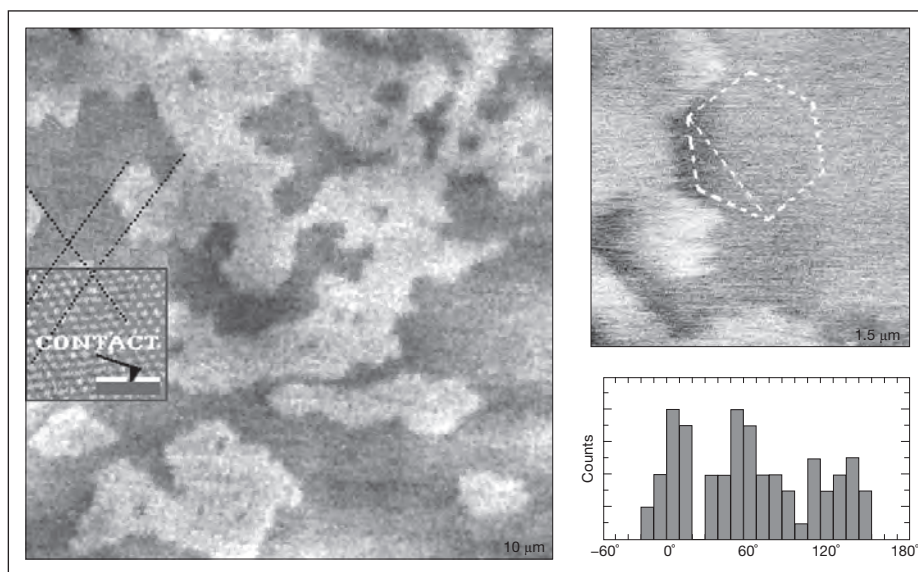


Figure 6. Scanning Polarization Force Microscopy (SPFM) images of structures formed by water on mica. Bright areas correspond to a second water layer and dark areas to the first water layer. The boundaries tend to be polygonal in shape, as shown in the smaller image where a hexagon is drawn for visual reference. The directions are strongly correlated with the mica lattice. The inset in the large image shows a contact AFM image obtained after the SPFM images, which provides a reference for angle measurements. The histogram shows the angles of the water-film boundaries relative to the mica lattice. (Adapted from Ref. [25]).

when released into the atmosphere, would trigger condensation of water from clouds and induce rain.

Materials that have crystal structures commensurate with one of the faces of  $I_h$  ice, such as the (111) face of  $BaF_2$  and some metals, have always been considered good candidates. However, it has been proven that having a close commensurability to the basal plane of ice is not a sufficient condition to promote ice nucleation. On other surfaces such as mica and amorphous silicon oxide, a very thin ice-like layer is thought to grow at temperatures above  $0^\circ\text{C}$ . Here we will review some SPFM experiments performed on mica to study the structure of water films as an example of a substrate that forces the water molecules to form structures different from what is expected from bulk water in the same conditions.

Mica is a layered aluminosilicate mineral commonly found in soils. One of the most common forms is Muscovite mica. The aluminosilicate layers are charged due to excess negative charge on the tetrahedrally coordinated  $Al^{3+}$  ions that substitute  $Si^{4+}$  in the  $SiO_2$  tetrahedra. Alkali ions are located between the  $(Al,Si)O_2$  layers to compensate for this charge. Upon cleavage, these ions become exposed to air. The freshly cleaved surface shows large, atomically flat terraces and it is therefore an ideal substrate for fundamental studies of water adsorption. The surface of mica is hydrophilic, and water spreads readily on a freshly prepared surface.

SPFM experiments at room temperature found that the presence of a water film on the mica surface changes the electrostatic force between tip and surface and modifies the contact potential [25]. A brief contact between an AFM tip and the surface is known to induce capillary condensation of water and the formation of a water neck around the contact point. On mica, after the tip is retracted, some excess water is left on the surface forming molecularly thin islands and droplets that can be imaged by SPFM. These structures were found to be metastable and disappeared by evaporation after seconds or a few minutes, depending on the humidity level of the environment. The islands were interpreted as a second water layer on the monolayer film already adsorbed on the mica surface.

When observing the islands it was found that their boundaries were often polygonal, forming angles of  $60^\circ$  and  $120^\circ$  (see Figure 6). By comparing SPFM images with contact images of the mica lattice it was found that the directions of the boundaries were related to the mica crystallographic directions. Based on this observation it was suggested that the molecularly thin water film has a solid, ice-like structure, in epitaxial relationship with the substrate.

Molecular Dynamics (MD) simulations of the water-mica system found that, at the monolayer coverage, water forms a two-dimensional H-bonded network in epitaxial relationship with the mica lattice [26], in line with the SPFM experimental findings. The simulations also predicted that there are no free OH bonds pointing out from the surface. Each H atom in the film is part of an H-bond with another water molecule or with oxygen atoms of the substrate. The absence of free H-bonds at the surface of the water monolayer implies that there is a net dipole moment with the positive end pointing towards the mica surface.

This prediction was confirmed by KPM experiments, where the surface potential of mica was measured as a function of relative humidity [27]. It was found that the contact potential of the mica substrate decreases by about 400 mV from its value under dry conditions ( $<10\%$  RH) when the humidity increases to 30%. After this decrease the potential remains nearly constant up to 80% RH. Above 80% RH the surface potential increased and became more positive, as shown in Figure 7. This is in line with the MD model where the first water layer has no free OH pointing out from the surface and should therefore have a negative surface potential relative to dry mica. When multilayers are formed, at 80%RH, free OH groups with the H pointing out are then present increasing the surface potential.

We have seen that at room temperature the growth of multilayers produces an increase in surface potential (more positive) compared to the surface potential of the monolayer. Interestingly, at temperatures below  $0^\circ\text{C}$ , the surface potential changes in the opposite direction, i.e., it becomes more negative above 80% RH (see Figure 7). This suggests that below  $0^\circ\text{C}$



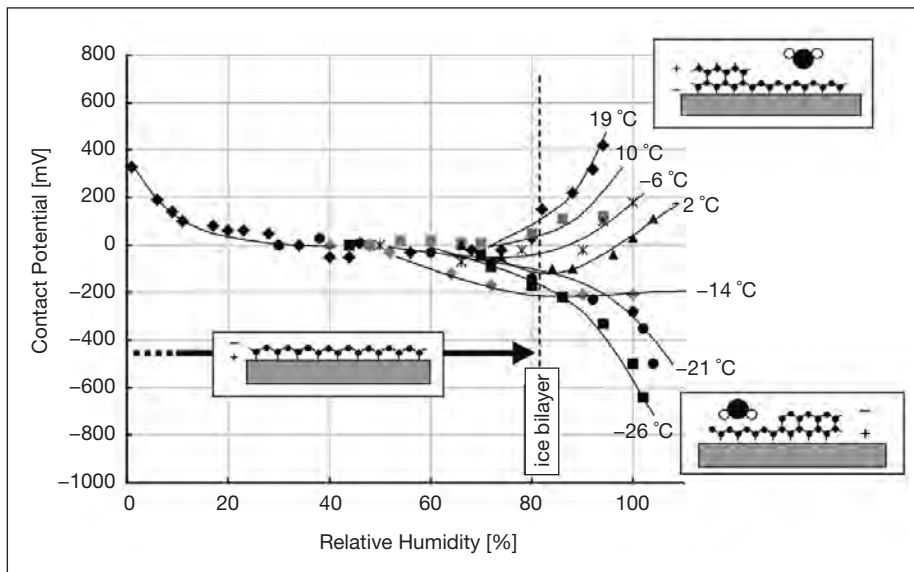


Figure 7. Changes in the contact potential of a mica surface relative to a hydrophobic tip versus relative humidity (RH) and for different temperatures. At room temperature the potential first decreases by about 400mV. This change can be explained by the orientation of water in the first monolayer, which has an average dipole moment pointing towards the surface. At ~20-30% RH it reaches a plateau and remains approximately constant until about 80% RH. At higher humidity the potential increases again. The observation is explained by a change in orientation of water in the second layer, where H from dangling H-bonds point upwards to the vapor phase. Below 0 °C the change in potential above 80% RH is reversed and becomes negative. This suggests that in that case the dipole-down orientation of water in the first layer continues in subsequent layers. (Adapted from Ref. [27]).

the water layers on top of the first layer grow with the positive end of the net dipole moment on average oriented towards the mica substrate, implying the growth of a ferroelectric water layer. The electrostatic energy accumulated in such dipole-oriented films makes them metastable and they revert to a dipole-disordered structure as the thickness increases beyond a few layers. KPM experiments on silicon oxide also found an oriented structure of the adsorbed water film up to 5 monolayers. In that case the orientation was with the net dipole moment oriented out from the silicon oxide surface [6].

### Chemistry reactions in water films (water on NaCl)

Sea-salt particles are formed by wave action and thrown up from the oceans to the atmosphere. These particles, mainly NaCl, are one of the most abundant particles in the atmosphere. Water coating the surfaces of sea particles affects their chemical reactivity with the molecules present in the troposphere. This reactivity strongly affects the chemistry of the most important pollutants in the troposphere such as ozone, N oxides and S oxides [28]. These reactions involve mainly Cl ions from the salt crystal that adsorbed water exposes to the reaction with those molecules. This mechanism is not yet well understood at molecular level. This is crucial to control the air quality in marine and coastal areas where the concentration of these particles in the troposphere is especially relevant.

Different AFM studies have examined the role of water on the cleavage faces of alkali halides (NaCl, KCl, KBr, KI) [29]. They found that there is a characteristic relative humidity value (CRH) that separates two water adsorption regimes related to the morphological modifications of the faces. Below CRH, the adsorption of water primarily affects the steps, very small changes in step morphology are observed and solvated ions remain localized in the vicinity of the steps with low mobility. Humidity higher than CRH produces large scale modifications of the step morphology and a high ionic surface mobility (Figure 8). Adsorption isotherms on NaCl (100) calculated from infrared

spectra, indicate that CRH corresponds approximately to the completion of the first water monolayer [4].

Most of these AFM experiments have been focused on the study of surface modifications and step movements occurring above CRH. Below CRH the modifications of the surface are almost unappreciable. However, to understand the role of water on NaCl surfaces it is important to understand the initial stages of water adsorption, i.e. below CRH.

Experiments using SPFM on NaCl (100) have shown that even below the CRH there is an increase in the electrostatic

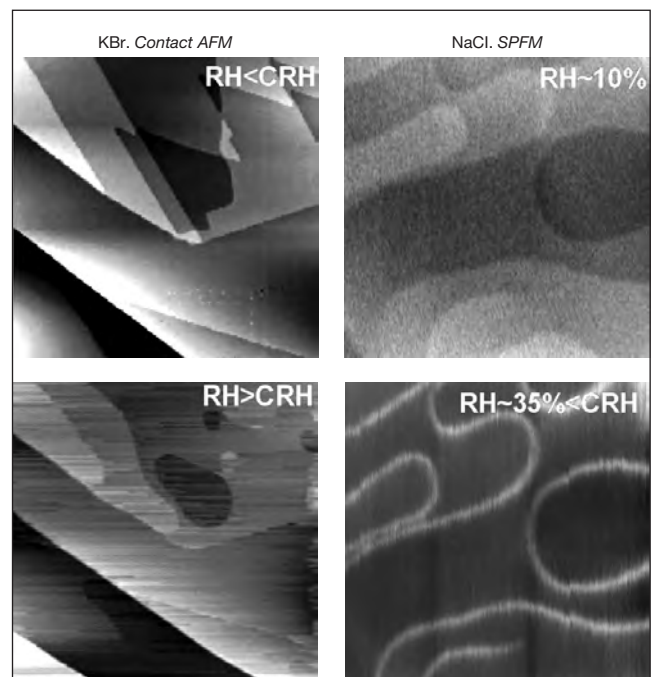


Figure 8. Left: Contact AFM images of KBr at low (top) and high humidity (bottom) relative to the CHR. Large scale modifications of the step morphology are observed for humidities higher than CRH. Right: SPFM images of NaCl acquired at different relative humidity (RH) values. The image at the top corresponds to RH = 10%. The bottom image at 35% RH shows a large enhancement of the step contrast due to mobility of solvated ions at the steps. Both images were acquired below CRH for NaCl, i.e. 40% RH. (Adapted from Ref. [29] and Ref.[30])



polarization force near steps (see Figure 8) [30]. This increase in polarization is related to the mobility of solvated ions in the vicinity of steps. This mobility can be measured by the frequency dependence of the electrostatic force between the tip and the surface, in the range of kHz. Previous SPFM experiments have studied the changes in the response time of the solvated ions as a function of relative humidity. They found a substantial change in the rate of increase of ionic mobility when the humidity was increased above CRH. Changes in the contact potential of the surface with relative humidity have also found important differences below and above the CRH. Below the CRH the contact potential on NaCl(100) was found to be different on the steps compared to the terraces (Figure 9). This was explained

by the formation of dipoles at the steps resulting from the preferential solvation of anions. As the RH increases, the contact potential on both terraces and steps becomes more negative but the difference between steps and terraces decreases and disappears completely at CRH, as shown in Figure 9. It has been also reported that when alkali halide surfaces are exposed to humidities above CRH, irreversible changes in the ionic distribution take place, so that when the surface is dried the original distribution is not recovered [31].

An important number of theoretical studies have been performed to try to understand the adsorption of water on NaCl(100). DFT calculations have shown that, for a coverage of one monolayer, water adsorption is favored on top of the Na ions [32]. The most favorable configuration is one with the molecular plane parallel to the surface. It was also found that below one monolayer, three dimensional water clusters can form. Recent theoretical analyses of the energetics of a water monolayer on NaCl have found that Cl ions can be lifted from the crystal surface with a negligible cost in energy and even reaching a minimum energy at  $\sim 2.4 \text{ \AA}$  from the surface [33]. The formation of a dipole on the surface due to the lifting of the Cl ions is in line with the contact potential measurements.

Based on all these results the following model for water adsorption on alkali halide surfaces was proposed. Below CRH water adsorbs preferentially at the step edges, where it solvates ions. Anions appear to solvate preferentially in the case of NaCl(001) and probably other salts although the type of ion that solvates first can depend on the history of water exposure and impurities in the crystal. The solvated anions give rise to a negative potential relative to the surface and are mobile along the steps. The increased ionic mobility gives rise to a stronger electrostatic force that produces the contrast enhancement observed in the SPFM topographic images. At CRH and higher humidity, both cations and anions solvate at similar rates removing the imbalance in the sign of contact potential. This triggers large scale motion of the steps and eliminates the contact potential difference between steps and terraces that is present at low humidity. The lift of the Cl ions due to water adsorption makes them easily accessible by molecules present in the environment to react with them.

### Avoiding wetting (water and SAMs)

Self-assembled monolayers (SAMs) have received much attention since they were discovered. From the technological point of view, the lubricant and antistiction properties of SAMs are especially important in micro electro mechanical (MEMS) and nano electro mechanical (NEMS) devices [34]. Despite its scientific importance and technological implications, the interaction of water with surfaces covered by SAMs is poorly understood.

Much work on the effect of humidity on the friction and adhesion properties of SAMs has been performed on surfaces completely covered by a SAM film. In these studies it was found that in general alkane SAM films constitute an excellent barrier to water adsorption due to their highly hydrophobic nature [35].

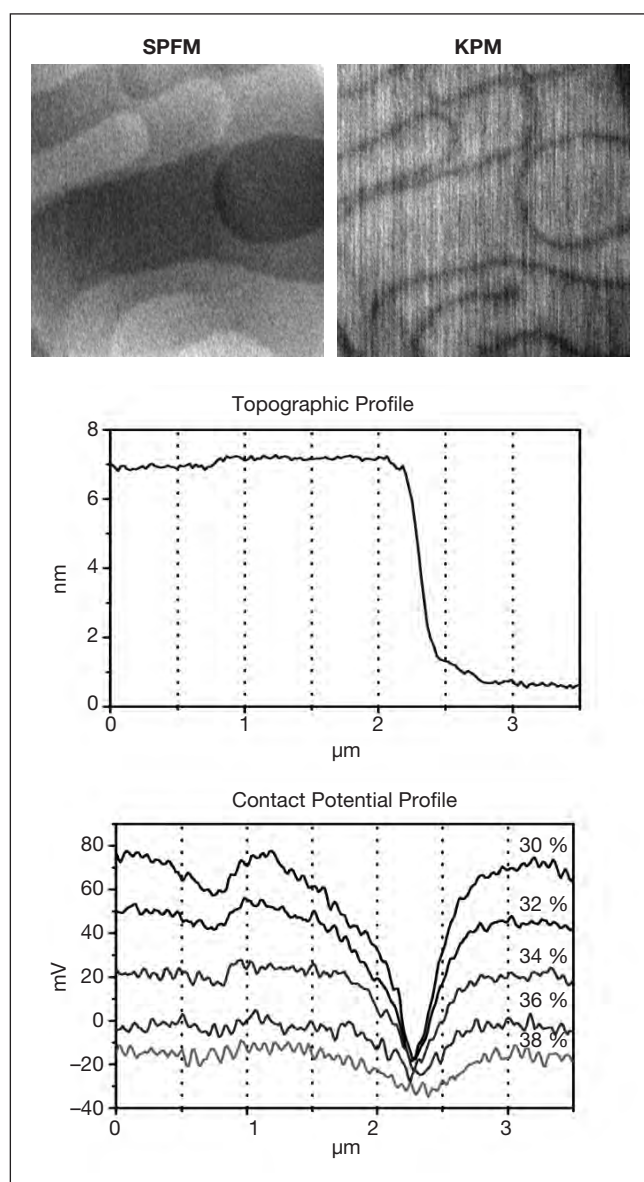


Figure 9. Top: SPFM (left) and contact potential (right) images acquired at RH = 25%. The KPM image shows a difference in contact potential between steps and terraces. Middle: topographic profile of a multiple step of 6.5 nm and a monoatomic step at 30% RH. Bottom: Kelvin Probe profiles of the same area at different humidities. As humidity increases the contact potential shifts to more negative values, the difference between the terraces and the steps decreases. Contact potential shift is interpreted as a preferential  $\text{Cl}^-$  solvation for humidity lower than CRH. (Adapted from Ref. [30]).

This hydrophobic nature is a consequence of the methyl terminal group at the SAMs. Other possible terminal groups such as amine or acid groups would produce a hydrophilic layer. The role of defects in the SAM such as pinholes, partially covered areas, etc. is difficult to determine. These defects appear especially for non-perfectly flat surfaces where a SAM is unable to perfectly follow the roughness of the surface.

SPFM studies of alkylsilane SAMs on mica found that complete alkylsilane monolayers were effective in blocking water adsorption [36]. On defective or incomplete layers however it was found that water dramatically influences the dielectric and contact potential properties of the surface.

In the previous section we have shown that on bare mica, water forms a layer with the average dipole moment oriented toward the surface when the humidity is between 30% and 80%, observed by the decrease in surface potential. We can also test the mobility of ions on the mica surface, as we described in the section devoted to ion mobility on NaCl. It was shown that ions present on the surface of mica become increasingly mobile by water adsorption. None of these effects was observed when a complete SAM was formed on mica. There are two possible explanations for this. One is that the molecular film is impermeable and that water cannot adsorb to or penetrate the mica interface. Another possibility is that water does penetrate the alkylsilane film but ionic mobility is suppressed at the interface. The contact potential of a complete SAM film does not change with humidity, as opposed to what is found when water adsorbs on mica. This finding seems to indicate that the molecular film is impermeable.

For partial alkylsilane films a contrast reversal in SPFM images was found near 40% RH (Figure 10). SPFM, as discussed above, contains both topographic and polarizability (dielectric constant) information. The ion mobility on mica can explain this observation: above 40% RH the ionic mobility is high enough in the uncovered mica regions for them to behave as good ionic conductors increasing the electrostatic force there. On the other hand, the regions protected by alkylsilane islands remain insulating, and the electrostatic force is low.

The contact potential difference between silane islands and the surrounding mica is negative below 40% RH but decreases and becomes zero near 50% RH. After that the silane-covered regions become more positive than mica, with contrast reaching a maximum near 80% RH. This effect is primarily due to water adsorption on the mica regions, which causes the local surface potential to become increasingly negative due to the average orientation of the water molecule dipoles while nothing changes on the silane islands. On completion of the monolayer, near 80% RH, the potential shift saturates. The decrease in potential beyond this point is due to the growth of water multilayers, since the dipole orientation for multilayers generally points up, as already discussed in above.

An important finding is the observation of edge effects, visible in both SPFM and KPM images (see Figure 10). This provides some insight into water penetration under silane islands. Although water cannot penetrate through dense, well-packed silane film regions, it does penetrate to a limited extent at the edges of islands and near defects, where packing may be less

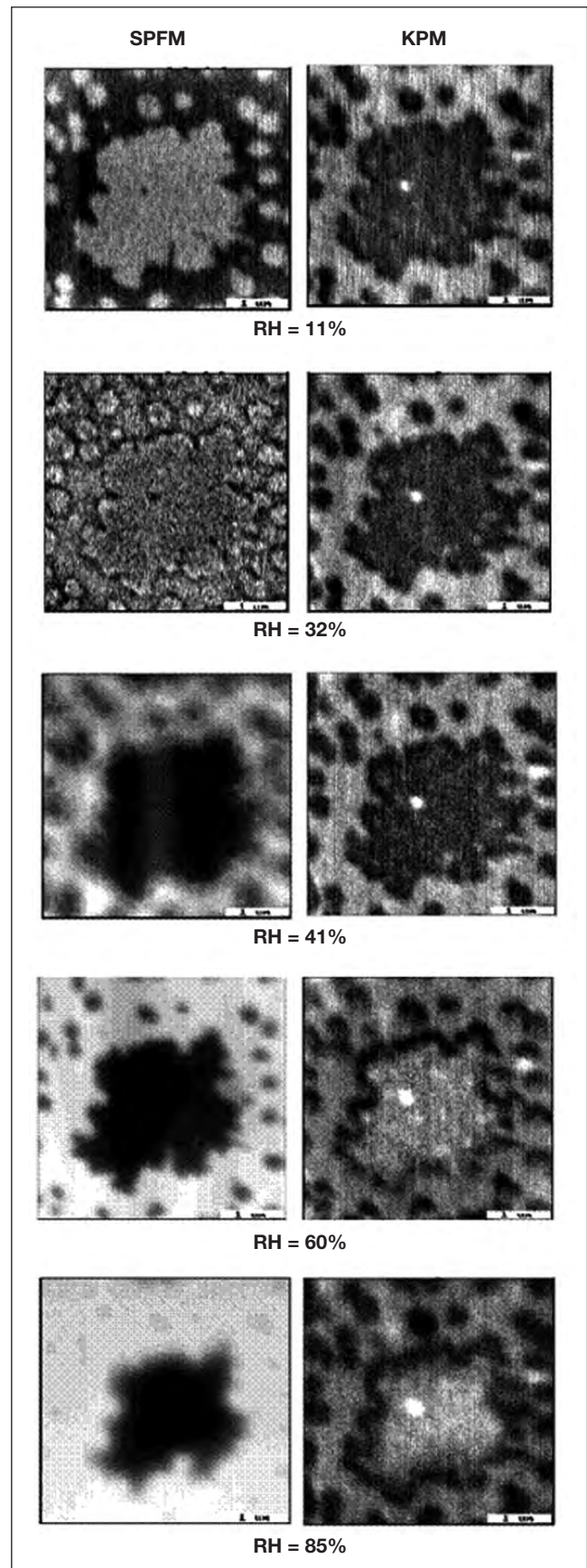


Figure 10. Series of SPFM and KPM images of hexadecylsilane islands on mica as a function of humidity. Note the contrast reversal in the SPFM images of the large island, from positive to negative, between 30% and 40% RH due to ion mobility on mica. At high humidity an edge effect can be observed in the Kelvin probe images of the large island. (Adapted from Ref. [36]).

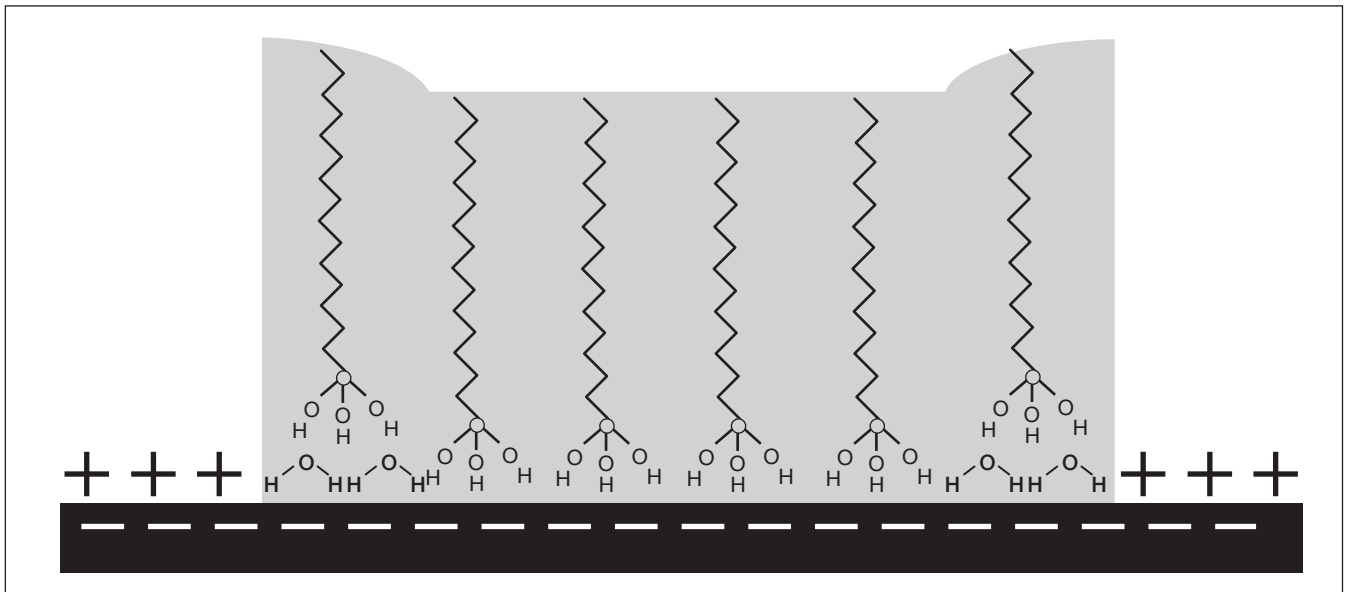


Figure 11. Schematic model of the water-silane monolayer interaction on a mica substrate. The negative contrast of the island relative to mica in this model is due to the displacement of the K ions by the molecules. The inserted water molecules around the island edge, with their dipole oriented downward, further decrease the surface potential. (Adapted from Ref. [36]).

than optimal. Bonding of the alkylsilane molecules to mica is only electrostatic and it would be easy for water molecules to penetrate between the molecule and the mica surface. Formation of H-bonded mica-water-silanol complexes, as shown in the schematic of Figure 11, may be responsible for the more negative contact potential of island borders relative to the island interior.

### Water nanostructures on surfaces (Water nanodroplets)

It is well known that when macroscopic liquid droplets form on a flat surface they adopt spherical cap shapes with a contact angle  $\theta$ . The contact angle is determined from the surface energies and the interaction forces between the liquid-solid interfaces. These forces will determine the wetting of the surface. In macroscopic droplets the dominant interactions are Van der Waals forces, present in every system but only dominant in non polar and inert atoms and molecules, and double layer forces originating from electrostatic and entropic interactions when surfaces become charged due to dissociation of surface ionic groups or adsorption of ions or dipoles from solution [37]. The latter is usually the dominant interaction for surfaces exposed to polar liquids like water. These phenomena have been studied for many years and contact angle measurements of droplets on the surface have been performed extensively.

There are other forces that come into play when the dimensions of the liquid film and droplets are in the nanometer range. In that case the size of the liquid molecules becomes an important factor. Short range oscillatory forces arise because the liquid molecules feel the presence of the walls of the substrate that forces them to form a layered structure near the interface. These forces are called structural or solvation forces and they decay exponentially with distance [37]. In water, solvation forces

are due not simply to molecular size effect but also, and most importantly, to the directional nature of the H-bonds between water molecules. These forces can be attractive or hydrophobic and repulsive or hydrophilic. They arise from the disruption or modification of the hydrogen-bonding water by the surfaces.

Other forces can also arise as a result of elastic strain of the growing film, which can be due to a surface ordering in the first few layers that reverts to the bulk liquid structure at larger distances. This elastic energy is stored in intermolecular distances and orientations that are stretched or compressed from the bulk values by the influence of the substrate at short distances. Similar phenomena are well known to occur in the growth of epitaxial layers in metals and semiconductors.

As we discussed earlier, in ambient conditions water films or droplets on a surface are of dimensions in the order of nanometers. It is therefore important to study the contact angle of droplets and film edges of submicrometer dimensions in order to understand wetting in these conditions.

Aqueous KOH solution droplets have been investigated on mica [38] and highly oriented pyrolytic graphite (HOPG) [39] using SPFM. These are model surfaces known to be hydrophilic and hydrophobic, respectively, and easy to prepare with large atomically flat terraces. The contact angle of the droplets was measured as a function of droplet height. They found a clear deviation from the macroscopic contact angle as the dimension of the droplet reduces due to the different role of solvation forces for small droplets, see figure 12.

On HOPG, the hydrophobic forces, which are attractive and exponentially dependent on the distances, clearly dominate. Therefore contact angle increases with droplet height. On mica the dependence of the contact angle on droplet height was much weaker than on graphite as expected from a surface with a weak hydrophobic interaction. Surprisingly contact angle still increases with droplet height, indicating the domination of hy-



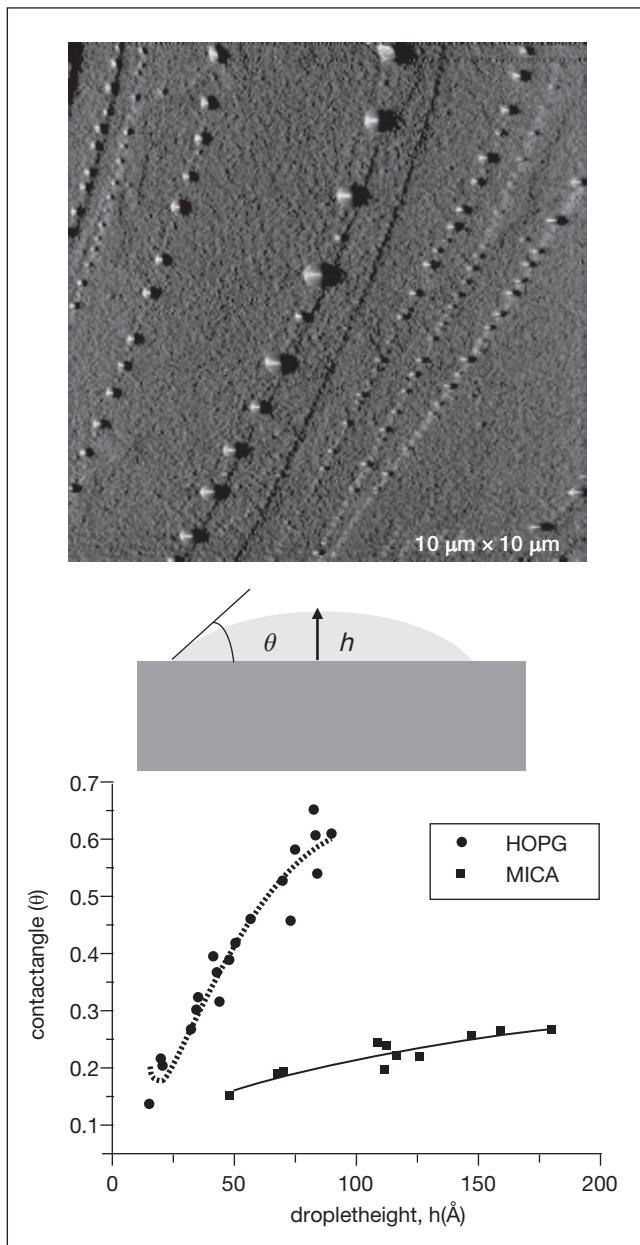


Figure 12. Top: SPFM image of droplets of an aqueous KOH solution deposited on an HOPG surface. Note that droplets preferentially attach to steps on the graphite surface. Bottom: Effective contact angle of the aqueous KOH droplets on HOPG and mica as a function of droplet height. (Adapted from Ref. [38] and Ref. [39].)

drophobic interactions for droplets of nanometer dimensions on a surface that at macroscopic level is considered hydrophilic.

Water nanodroplets (WNDs) can be also imaged with AFM by fixing them in nanobeakers [40]. Figure 13 shows the topography (a) and phase (b) images of a WND confined on a molecular nanobeaker. Water can be reversibly introduced into or removed from the nanobeakers by modifying RH, creating or destroying WND. In the image, the WND height is ca. 35 nm. Note the well-defined phase contrast defining the location of water in the line profile in Figure 13(b).

Taking advantage of the confinement of WNDs in nanobeakers, the exploration of their mechanical behavior becomes possible. WNDs behave like Hookean springs exhibiting force con-

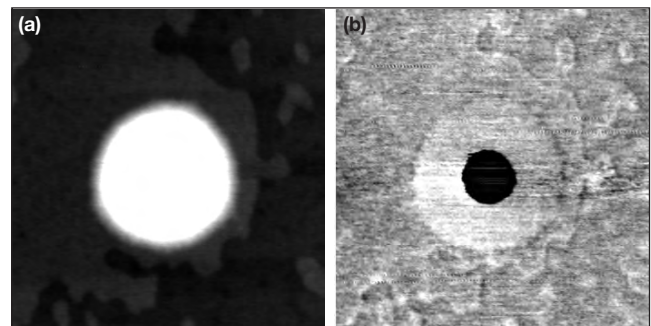


Figure 13. Tapping mode AFM image [ $1.0\ \mu\text{m} \times 1.0\ \mu\text{m}$ ] of a WND confined in a nanobeaker measured at RH  $\sim 50\%$ : (a) topography and (b) phase. (Adapted from Ref. [40]).

starts close to  $1\ \text{Nm}^{-1}$ , when forces in the nN range are applied to them with the tip of a cantilever. This value is significantly larger than the well-known surface tension value of  $0.073\ \text{Nm}^{-1}$ , an increase essentially due to the nanometric length scale involved. The increase in the surface tension of water with the reduction of the length scale has been experimentally evidenced i.e., by grazing-incidence X-ray scattering measurements using synchrotron radiation [41].

From the  $1\ \text{Nm}^{-1}$  force constant value an associated frequency for the WND of ca. 1 THz is obtained, which is in the spectral range where the collective modes of confined liquids are most evident [42]. In the example shown here, the contributions of both surface shape and internal compressional oscillations are involved. Hence, AFM force measurements can give an estimation of the weighted distribution of the collective modes of vibration of confined liquids. It is still unclear whether water molecules might promote a hydrogen-bond network at the nanodroplet-air interface generating an ice-like structure, as suggested for water films on mica [43].

## Summary

Scanning Probe Microscopies have led to a new approach to the study of water films and droplets on surfaces. Our understanding of the structure of water films in the nanometer range of thickness has advanced considerably over the last few years due to the intensive application of these experimental techniques. We have seen how STM at low temperatures has been used to study water adsorption on metals at low coverages. Using this technique it is possible to investigate the structure of the first water monolayer from the smallest clusters, dimers and trimers, to the basic structure for the formation of a monolayer, the hexamer. Different factors determine the structure of the water monolayer: the strength of the H-bonds between water molecules and the bonds between water molecules and the metal substrate, the mismatch between O-O distances in H-bonded water molecules and lattice constant of the metal and the possible dissociation of the water molecules. All interactions being in the same order, the effect of surface defects or the interaction with adsorbates may result in very different water structures. For example, studies of the adsorption of water on Ru(0001) show how important water clustering is for its dis-

sociation, and how the interaction with adsorbates such as C or O can enhance or completely inhibit dissociation.

At ambient temperatures we have seen how SPFM can be a powerful tool that makes it possible not only to image liquids on surfaces with a minimum perturbation of the films and droplets but also to obtain dielectric and contact potential information on the surface. SPFM has been used to study how the structure on the adsorbed water film imposed by the substrate extends beyond the water monolayer. On mica an ice-like film in epitaxial relationship with the mica surface has been observed up to the second monolayer of adsorbed water. In multilayer films the water molecules showed a highly oriented structure induced by the substrate.

The dielectric and contact potential information that can be obtained from SPFM experiments have been used to study chemical processes induced by water on the surface such as ion mobility or the formation of charges and dipoles, which are extremely important in chemical reactions that take place within the adsorbed water film. Studies of water adsorption on NaCl suggested a preferential solvation of the Cl ion at low humidity. These phenomena may be the clue to understanding atmospheric chemical reactions that take place within the water film on sea salt crystals.

From the technological point of view these techniques are used to study the wetting properties of nanofabricated devices where one of the main contributions to friction is due to capillarity phenomena. We have seen how SPFM has been used to investigate the quality of SAMs as a hydrophobic coating of surfaces to avoid adsorption of water. Although a complete layer has been tested as a good hydrophobic coating, water has been observed to penetrate through defects in a complete monolayer.

Finally we have seen that structural forces within the liquid become a crucial factor in the wetting of the surface when the droplets are in the nanometer range, showing different properties than those found in macroscopic droplets.

## Acknowledgements

A Verdaguer and A. Mugarza are supported by the program *Ramón y Cajal* of the *Ministerio de Educación y Ciencia*, Spain.

## References

- [1] Henderson M.A. (2002). The interaction of water with solid surfaces: fundamental aspects revisited. *Surf. Sci. Rep.* 46:1-308
- [2] Verdaguer A., Sacha G.M., Bluhm H., Salmeron M. (2006). The Molecular Structure of Water at Interfaces: Wetting at the Nanometer Scale. *Chem. Rev.*, 106 (4):1478-1510
- [3] Israelachvili J.N., Tandon R.K., White L.R. (1979). Measurement of forces between 2 mica surfaces in aqueous poly(ethylene oxide) solutions. *Nature*, 277:775-776
- [4] Ewing G.E. (2004). Thin film water. *J. Phys. Chem. B* 108(41):15953-15961
- [5] Bardon S., Ober R., Valignat M.P., Vandenbrouck F., Cazabat A.M., Daillant J. (1999). Organization of cyano-biphenyl liquid crystal molecules in prewetting films spreading on silicon wafers. *Phys. Rev. E.* 59(6):6808-6818
- [6] Verdaguer A., Weis Ch., Oncins G., Ketteler G., Bluhm H., Salmeron M. (2007). Growth and Structure of water on SiO<sub>2</sub> films on Si investigated by Kelvin probe microscopy and in situ X-ray Spectroscopies, *Langmuir* 23(19): 9699-9703
- [7] Samori P. (Ed). (2006). Scanning Probe Microscopies Beyond Imaging, Wiley-VCH, Weinheim.
- [8] Ho W. (2002). Single-molecule chemistry. *J. Chem. Phys.* 117:11033
- [9] Michaelides A., Ranea V.A., de Andres P.L., King D.A. (2003). General model for water monomer adsorption on close-packed transition and noble metal surfaces. *Phys. Rev. Lett.* 90(21):216102
- [10] Mitsui T., Rose M.K., Formin E., Ogletree D.F., Salmeron M. (2002). Water diffusion and clustering on Pd(111). *Science* 297:1850-1852
- [11] Shimizu T.K., Mugarza A., Cerdá J.I., Heyde M., Qi Y., Schwarz U.D., Ogletree D.F., Salmerón M. (2007). Identification of the species formed by water adsorption and dissociation on the Ru(0001) surface by scanning tunneling microscopy *J. Phys. Chem. C.* 112:7445-7454.
- [12] Michaelides A., Morgenstern K. (2007). Ice nanoclusters at hydrophobic metal surfaces. *Nature Materials* 6(8): 597-601.
- [13] Morgenstern K., Nieminen J. (2002). Intermolecular bond length of ice on Ag(111). *Phys. Rev. Lett.* 88(6):066102
- [14] Morgenstern K., Rieder K.H. (2002). Formation of the cyclic ice hexamer via excitation of vibrational molecular modes by the scanning tunneling microscope. *J. Chem. Phys.* 116(13):5746-5752
- [15] Cerda J., Michaelides A., Bocquet M.-L., Feibelman P.J., T. Mitsui T., Rose M.K., Formin E., Salmeron M. (2004). Novel water overlayer growth on Pd(111) characterized with scanning tunneling microscopy and density functional theory. *Phys. Rev. Lett.* 93(11):116101
- [16] Held G., Menzel D. (1994). The Structure of the ( $\sqrt{3}\times\sqrt{3}$ ) R30° bilayer of D<sub>2</sub>O on Ru(0001). *Surf. Sci.* 316:92-102
- [17] Feibelman P.J. (2002). Partial dissociation of water on Ru(0001). *Science* 295:99-102
- [18] Michaelides A., Alavi A., King D.A. (2003). Different Surface Chemistries of Water on Ru(0001): From Monomer Adsorption to Partially Dissociated Bilayers. *J. Am. Chem. Soc.* 125:2746
- [19] Faradzhev N.S., Kostov K.L., Feulner P., Madey T.E., Menzel D. (2005). Stability of water monolayers on Ru(0001): Thermal and electronically induced dissociation. *Chem. Phys. Lett.* 415:165
- [20] Tatar khanov M., Formin E., Salmeron M., Andersson K., Ogasawara H., Pettersson L.G.M., Nilsson A., Cerda J.I. (2008) The structure of mixed H<sub>2</sub>O-OH monolayer films on Ru (0001) *J. Chem. Phys.* 129(15)154109.
- [21] Clay C., Haq S., Hodgson A. (2004). Intact and dissociation

- tive adsorption of water on Ru(0001). *Chem. Phys. Lett.* 388:89
- [22] Gladys M.J., Mikkelsen A., Andersen J.N., Held G. (2005). Water adsorption on O-covered Ru(0001): Coverage-dependent change from dissociation to molecular adsorption. *Chem. Phys. Lett.* 414:311
- [23] Cabrera-Sanfeliu P., Arnau A., Mugarza A., Shimizu T.K., Salmeron M., Sánchez-Portal D. (2008) Decisive role of the energies of dissociation products in the adsorption of water on O/Ru (0001) *Phys. Rev. B* 78:155438.
- [24] Hu J., Xiao X.D., Salmeron M. (1995). Scanning Polarization Force Microscopy — a technique for imaging liquids and weakly adsorbed layers. *Appl. Phys. Lett.* 67:476-478
- [25] Hu J., Xiao X.D., Ogletree D.F., Salmeron M. (1995). Imaging the condensation and evaporation of molecularly thin-films of water with nanometer resolution. *Science* 268:267-269. Salmeron M., Xu L., Hu J. (1997). High-resolution imaging of liquid structures: Wetting and capillary phenomena at the nanometer scale. *MRS Bull* 22:36-41
- [26] Odelius M., Bernasconi M., Parinello M. (1997). Two dimensional ice adsorbed on mica surface. *Phys. Rev. Lett.* 78:2855-2858
- [27] Bluhm H., Inoue T., Salmeron M. (2000). Formation of dipole-oriented water films on mica substrates at ambient conditions. *Surf. Sci.* 462(1-3):L599-L602
- [28] Finlayson-Piits B.J. (2003). The Tropospheric chemistry of sea salt: A molecular-level view of the chemistry of NaCl and NaBr. *Chem. Rev.* 103:4801-4822
- [29] Luna M., Rieutord F., Melman N.A., Dai Q., Salmeron M. (1998). Adsorption of water on alkali halide surfaces studied by scanning polarization force microscopy. *J. Phys. Chem. A.* 102:6793-6800
- [30] Verdaguer A., Sacha G.M., Luna M, Ogletree D.F., Salmeron M. (2005). Initial stages of water adsorption on NaCl (100) studied by scanning polarization force microscopy. *J. Chem. Phys.* 123(12):124703
- [31] Ghosal S., Verdaguer A., Hemminger J.C., Salmeron M. (2005). In situ study of water-induced segregation of bromide in bromide-doped sodium chloride by scanning polarization force microscopy. *J. Phys. Chem. A.* 109(21): 4744-4749
- [32] Park J.M., Cho J.-H., Kim K.S. (2004). Atomic structure and energetics of adsorbed water on the NaCl(001) surface. *Phys. Rev. B.* 69:233403
- [33] Cabrera-Sanfeliu P., Sánchez Portal D., Verdaguer A., Darling G.R., Salmeron M., Arnau A. (2007). Spontaneous Emergence of Cl<sup>-</sup> Anions from NaCl(100) at Low Relative Humidity. *J. Phys. Chem. C.* 111(22):8000-8004
- [34] Maboudian R., Carraro C. (2004). Surface chemistry and tribology of MEMS. *Ann. Rev. Phys. Chem.* 55:35-54
- [35] Qian L.M., Tian F., Xiao X.D. (2003). Tribological properties of self-assembled monolayers and their substrates under various humid environments. *Tribol. Lett.* 15(3):169-176
- [36] Diez-Perez I., Luna M., Teheran F., Ogletree D.F., Sanz F., Salmeron M. (2004). Interaction of water with self-assembled monolayers of alkylsilanes on mica. *Langmuir* 20(4):1284-1290
- [37] Israelachvili J. (1985). *Intermolecular and Surface Forces.* Academic Press, New York
- [38] Rosoff M. (Ed). (2001). *Nano-Surface Chemistry*, Chap: 6. Marcel Dekker, INC. New York
- [39] Hu J., Carpick R.W., Salmeron M., Xiao X.D. (1996). Imaging and manipulation of nanometer-size liquid droplets by scanning polarization force microscopy. *J. Vac. Scien. Tech. B.* 14(2):1341-1343
- [40] Fraxedas J., Verdaguer A., Sanz F., Baudron S., Batail P. (2005). Water nanodroplets confined in molecular nanobeakers. *Surf. Sci.* 588(1-3):41-48
- [41] Fradin C., Braslau A., Luzet D., Smilgies D., Alba M., Boudet N., Mecke K.; Daillant J. (2000). Reduction in the surface energy of liquid interfaces at short length scales. *Nature* 403:871-874
- [42] Tamura A., Ichinokawa T. (1984). Liquid-drop model of a small particle in a liquid-state. *Surf. Sci.* 136:437-448
- [43] Miranda P.B., Xu L., Shen Y.R., Salmeron M. (1998). Ice-like water monolayer adsorbed on mica at room temperature. *Phys. Rev. Lett.* 81(26):5876-5879

## About the authors

**Albert Verdaguer** was born in 1971 in Vic, Catalonia. He studied physics at the Universitat de Barcelona. He received his Ph.D in physics in 2001 after completing his thesis work in computer simulation of liquids under the direction of Prof. Joan-Àngel Padró at the Universitat de Barcelona. He spent two years as a member of staff at the Nanometric Techniques Unit of the Scientific-Technical Services of the Universitat de Barcelona using scanning force microscopy in a wide range of different studies. From 2003 to 2006 he was a

postdoctoral research fellow in Dr. M. Salmeron's laboratory at the Lawrence Berkeley National Laboratory. He is currently at the Institut Català de Nanotecnologia as a Ramon y Cajal researcher. His research interests include the interaction of water with surfaces under ambient conditions and the interaction of atmospheric gases with salt crystal surfaces.

**Aitor Mugarza** was born in 1974 in Oñati, in the Basque Country. He graduated in Physics from the Euskal Herriko Unibertsitatea – Universidad del País Vasco in 1997 and obtained his PhD in 2002 at the same university, under the direc-

tion of Prof. Jose Enrique Ortega and based on the electronic structure of low dimensional systems studied by angle-resolved photoemission spectroscopy using synchrotron radiation. From 2003 to 2006 he was as a postdoctoral research fellow in Dr. Miquel Salmeron's group at Lawrence Berkeley National Laboratory, where he worked on the construction of a low temperature scanning tunneling microscope (LT-STM) and its application to single-molecule manipulation and spectroscopy. At the present he is a Ramon y Cajal researcher at the Institut Català de Nanotecnologia. His gener-



*al research areas of interests are surface science and nanoscience, focusing in the electronic and vibrational properties of single molecules or atoms and their interaction with the substrate and other surface molecules studied by LT-STM.*

**Jordi Fraxedas** (Tarragona, 1962) graduated in Physics from the Universidad de Zaragoza in 1985 and obtained his PhD (Dr. rer. nat.) in 1990 at the Uni-

*versity of Stuttgart (Germany). His Thesis work was performed at the Max Planck Institut für Festkörperforschung and at the Berliner Speicherring für Synchrotronstrahlung (BESSY) under the supervision of Prof. Dr. M. Cardona. After a post-doctoral position at the European Synchrotron Radiation Facility (ESRF) in Grenoble (France) and an Established Researcher position at the European*

*Laboratory for Particle Physics (CERN) in Geneva (Switzerland) he is now a tenured scientist at the Institut de Ciència de Materials de Barcelona (ICMAB) and at the Centre d'Investigació en Nanociència i Nanotecnologia (CIN2) of the Consejo Superior de Investigaciones Científicas (CSIC). His research interests include surface science, nanoscience and molecular organic materials.*